Synthesis and Characterization of Temperature-Sensitive Block Copolymers from Poly(*N*-isopropylacrylamide) and 4-Methyl-ε-caprolactone or 4-Phenyl-ε-caprolactone

Ren-Shen Lee, Yi-Ting Huang, Wen-Hsin Chen

The Center of General Education, Chang Gung University, Kwei-Shan, Tao-Yuan 333, Taiwan, Republic of China

Received 20 December 2009; accepted 1 April 2010
DOI 10.1002/app.32546
Published online 3 June 2010 in Wiley InterScience (www.interscience.wiley.com).

ABSTRACT: This study synthesizes thermally sensitive block copolymers poly(*N*-isopropylacrylamide)-*b*-poly(4-methyl-ε-caprolactone) (PNIPA-*b*-PMCL) and poly(*N*-isopropylacrylamide)-*b*-poly(4-phenyl-ε-caprolactone) (PNIPA-*b*-PBCL) by ring-opening polymerization of 4-methyl-ε-caprolactone (MCL) or 4-phenyl-ε-caprolactone (BCL) initiated from hydroxy-terminated poly(*N*-isopropylacrylamide) (PNIPA) as the macroinitiator in the presence of $SnOct_2$ as the catalyst. This research prepares a PNIPA bearing a single terminal hydroxyl group by telomerization using 2-hydroxyethanethiol (ME) as a chain-transfer agent. These copolymers are characterized by differential scanning calorimetry (DSC), ^{1}H-NMR, FTIR, and gel permeation chromatography (GPC). The thermal properties (T_g) of diblock copolymers depend on polymer compositions. Incorporating larger amount of MCL or BCL into the macromolecular backbone decreases T_g. Their solutions show transparent below a lower critical solution temperature (LCST) and opaque above the LCST. LCST values for the PNIPA-*b*-PMCL aqueous solution were observed to shift to lower temperature than that for PNIPA homopolymers. This work investigates their micellar characteristics in the aqueous phase by fluorescence spectroscopy, transmission electron microscopy (TEM), and dynamic light scattering (DLS). The block copolymers formed micelles in the aqueous phase with critical micelle concentrations (CMCs) in the range of 0.29–2.74 mg L^{-1}, depending on polymer compositions, which dramatically affect micelle shape. Drug entrapment efficiency and drug loading content of micelles depend on block polymer compositions. © 2010 Wiley Periodicals, Inc. J Appl Polym Sci 118: 1634–1642, 2010

Key words: temperature-sensitive; amphiphilic block copolymer; PNIPA-b-PM(B)CL

INTRODUCTION

During the past decade, various fields have focused considerable attention on stimuli-responsive polymers.[1] Because of their sensitivity to environment changes, they can be used in areas such as drug delivery, tissue engineering, biosensing, and separation processes.[2–4] Although there are many stimuli such as temperature, pH, light, or electric field, more studies have focused on temperature- and/or pH-responsive materials for the biomedical applications.[5–7]

The most widely used intelligent polymers for temperature sensitivity are poly(*N*-isopropylacrylamide) (PNIPA) and its related copolymers. PNIPA shows a reversible coil-to-globule transition at about 32°C (lower critical solution temperature, LCST), and is well soluble in water below the LCST. However, when the temperature increases above the LCST, the polymer becomes insoluble and precipitates out from its aqueous solution. Changing the hydrophilicity/hydrophobicity balance in the copolymer adjusts its LCST. The LCST appropriately elevated or reduced by copolymerizing NIPA with a more hydrophilic monomer or a more hydrophobic monomer.[8]

However, these thermosensitive micelles are nondegradable, raising questions on elimination of micelles from the body after its use. For this purpose, this study copolymerizes thermo-responsive PNIPA segments with hydrophobic biodegradable segments such as poly(DL-lactic acid) (PDLLA),[9–12] poly(lactic-*co*-glycolic acid) (PLGA),[13] or poly(ε-caprolactone) (PCL).[14–16] Results demonstrate that these micelles have a slow rate of drug release at temperatures below the LCST but rapidly release the encapsulated drug upon heating to above the LCST.

This study focuses on the PNIPA-*b*-PMCL and PNIPA-*b*-PBCL diblock copolymers. The hydrophobic PMCL and PBCL blocks are a well-known biodegradable polyester.[17] The PNIPA block may compose as hydrophilic corona of the PNIPA-*b*-PMCL and PNIPA-*b*-PBCL nanoparticles acting as a temperature sensitive component. Therefore, this study expects that the PNIPA-*b*-PMCL and PNIPA-*b*-PBCL

Correspondence to: R.-S. Lee (shen21@mail.cgu.edu.tw).
Contract grant sponsor: National Science Council; contract grant number: 97-2221-E-182-009.
Contract grant sponsor: Chang Gung University; contract grant number: BMRP 123.

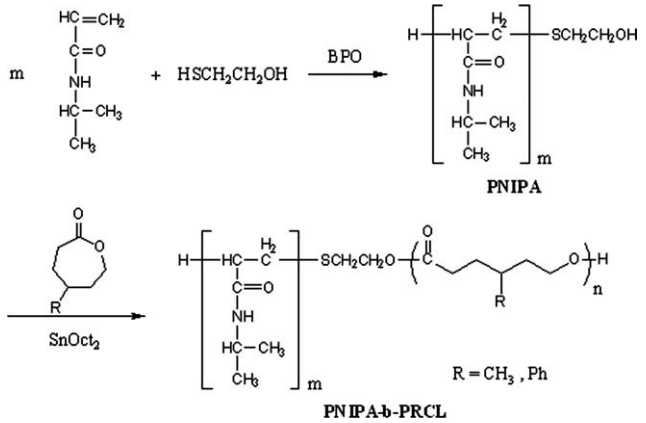

Scheme 1 Synthesis of PNIPA-*b*-PRCL block copolymers.

nanoparticles might form core-shell type polymeric self-aggregates with thermosensitive nanoparticle corona. For detailed investigation, this research synthesizes PNIPA-*b*-PMCL and PNIPA-*b*-PBCL diblock copolymers with different substituted PCL block lengths. Then, we prepare the thermo-sensitive PNIPA-*b*-PMCL and PNIPA-*b*-PBCL nanoparticles by a dialysis method and investigate their physicochemical characteristics and thermosensitives. Finally, the investigation examines the efficacies of PNIPA-*b*-PMCL and PNIPA-*b*-PBCL nanoparticles as drug carriers with the hydrophobic indomethacin model drug.

EXPERIMENTAL

Materials

N-Isopropylacrylamide (NIPA), 2-mercaptoethanol (ME), benzoyl peroxide (BPO), 4-methylcyclohexanone, 4-phenylcyclohexanone, and pyrene were purchased from the Aldrich Chemical (Milwaukee, WI). *m*-Chloroperoxybenzoic acid (*m*-CPBA) and indomethacin was purchased from the Fluka Chemical (Buchs SGI, Switzerland). Stannous octoate ($SnOct_2$) was purchased from the Strem Chemical (Newburyport, MA). MCL and BCL were prepared according to the reported method.[18] Organic solvents such as tetrahydrofuran (THF), methanol, chloroform, *N*,*N*-dimethylformamide (DMF) and *n*-hexane with a high pressure liquid chromatography (HPLC) grade were purchased from the Merck Chemical (Darmstad, Germany). Ultrapure water was used by purification with a Milli-Q Plus (Waters, Milford, MA).

Synthesis of PNIPA-*b*-PMCL and PNIPA-*b*-PBCL diblock copolymers

The diblock copolymers with different contents and compositions were synthesized according to the method reported previously (Scheme 1).[14] Briefly, hydroxyl-terminated PNIPA precursor polymer was prepared by the radical copolymerization using BPO as an initiator and 2-hydroxyethanethiol as a chain transfer agent (CTA). For instance, *N*-isopropylacrylamide (4.2 g, 37.1 mmol), 2-hydroxyethanethiol (0.29 g, 3.71 mmol), and BPO (83.4 mg, 2 wt %) were dissolved in 15 mL of THF. The solution was degassed by bubbling with nitrogen for 20 min. The reaction mixture was refluxed for 24 h under nitrogen. Upon completion, the product was precipitated out by adding diethyl ether. A white powder PNIPA was obtained. The diblock copolymers of PNIPA-*b*-PMCL and PNIPA-*b*-PBCL were synthesized by the ring-opening esterification polymerization of MCL or BCL with the hydroxyl-terminated precursor in toluene using $SnOct_2$ as the catalyst. All monomers and precursor polymer should notably be dried at vacuum oven before reaction. The reaction mixture was refluxed in chlorobenzene for 24 h under nitrogen. Table I lists the properties of the resultant block copolymers. Figures 1 and 2 show the representative ^{1}H-NMR and FTIR spectra of PNIPA15 and PNIPA15-*b*-PMCL18.

Characterization

^{1}H-NMR spectra were recorded at 500 MHz (with a Bruker WB/DMX-500 spectrometer, Ettlingen, Germany) with chloroform ($\delta = 7.24$ ppm) as an internal standard in chloroform-*d* ($CDCl_3$). IR spectra were measured on a Bruker TENSOR 27 Fourier transform infrared (FTIR) spectrophotometer (Bruker, Germany). Samples were either neatly placed on NaCl plates or pressed into KBr pellets. A thermal analysis of the polymer was performed on a DuPont 9900 system, consisting of DSC (Newcastle, DE). The heating rate was 20°C min^{-1}. T_gs were read at the middle of heat capacity change and taken from the second heating scan after quick cooling. Number- and weight-average molecular weights (M_n and M_w, respectively) of the polymer were determined by a GPC system, carried out on a Jasco HPLC system equipped with a model PU-2031 refractive-index detector (Tokyo, Japan), and Jordi Gel polydivinyl benzene (DVB) columns with pore sizes of 100, 500, and 1000 Å. Chloroform was used as the eluent at a flow rate of 0.5 mL min^{-1}. PEG standards with a low dispersity (Polymer Sciences) were used to generate a calibration curve. Data were recorded and manipulated with a Windows-based software package (Scientific Information Service). UV-vis spectra were obtained using a Jasco V-550 spectrophotometer (Tokyo, Japan). The pyrene fluorescence spectra were recorded on a Hitachi F-4500 spectrofluorometer (Japan). Square quartz cells of 1.0 cm × 1.0 cm were used. For fluorescence excitation spectra, the detection wavelength (λ_{em}) was set at 390 nm.

TABLE I
Results of the Block Copolymerization of Substituted ε-Caprolactone (4-R-ε-CL) Initiated with Hydroxyl-Terminated PNIPA[a]

Copolymer	[4-R-ε-CL]/[PNIPA] Molar ratio in the feed	[4-R-ε-CL]/[PNIPA] Molar ratio[b]	W_{PNIPA} (%)[c]	Yeild (%)	$M_{n,GPC}$[d]	M_w/M_n[d]	$M_{n,NMR}$[e]	$M_{n,th}$[f]	T_{g1} (°C)[g]	T_{g2} (°C)[g]
PNIPA15-*b*-PCL11	15/1	11/1	0.6	63	3420	1.45	3030	3480		
PNIPA 15-*b*-PMCL9	15/1	9/1	0.8	80	2330	1.52	2950	3690	30.8	83.7
PNIPA 15-*b*-PMCL18	30/1	18/1	0.6	54	2980	1.48	4100	5640	24.7	
PNIPA 15-*b*-PMCL32	50/1	32/1	0.4	45	5030	1.55	5900	8200	−55.3	
PNIPA 15-*b*-PMCL45	70/1	45/1	0.3	51	6320	1.26	7560	10760	−55.6	
PNIPA 7-*b*-PMCL46	50/1	46/1	0.2	55	5050	1.92	5220	7270	−56.8	
PNIPA 15-*b*-PBCL13	50/1	13/1	0.8	70	2290	1.57	3510	11300	5.8	44.7
PNIPA 7-*b*-PBCL34	50/1	34/1	0.2	72	3550	1.98	9610	10370	10.6	

[a] $M_{n,NMR}$ was 870 for PNIPA7 and 1800 for PNIPA15.
[b] Determined by ^{1}H-NMR spectroscopy.
[c] W_{PNIPA}: weight fraction of hydrophilic segment PNIPA.
[d] Determined by GPC.
[e] Determined by ^{1}H-NMR spectroscopy of PNIPA-*b*-PRCL.
[f] $M_{n,th} = M_{n,NMR} + M_{4\text{-R-}\varepsilon\text{-CL}} \times [M]/[I]$ (where $M_{n,NMR}$ i.e., the number-average molecular weight of PNIPA, $M_{4\text{-R-}\varepsilon\text{-CL}}$ is the molecular weight of 4-R-ε-CL, [M] is the monomer molarity concentration, and [I] is the macroinitiator molarity concentration).
[g] Determined from DSC thermograms.

Optical transmittance measurements

The experiment measured optical transmittance of aqueous polymer solution (5 mg mL^{-1}) at various temperatures at 500 nm with a UV-vis spectrometer (Jasco V-550, Japan). Sample cells were thermostated with a temperature-controller (Jasco ETC-505T, Japan). Heating rate was 0.1°C min^{-1}. The LCST values of polymer solutions were determined at the temperatures showing an optical transmittance of 90%.

Measurements of fluorescence spectroscopy

To prove micelles formation, fluorescence measurements were carried out using pyrene as a probe.[15] Fluorescence spectra of pyrene in aqueous solution were recorded at room temperature on a fluorescence spectrophotometer. The sample solutions were prepared by first adding known amounts of pyrene in acetone to a series of flasks. After the acetone evaporated completely, measured amounts of micelle solutions with various concentrations of PNIPA-*b*-PMCL ranging from 0.037 to 75 mg L^{-1} were added to each flask and mixed by vortexing. The pyrene concentration in the final solutions was $6.1 \times 10^{-7}M$. The flasks were allowed to stand overnight at room temperature to equilibrate the pyrene and the micelles. The emission wavelength was 390 nm for excitation spectra.

Preparation of polymeric micelles

Polymeric micelles of PNIPA-*b*-PMCL copolymers were prepared using the dialysis method.[19] Briefly, a solution of PNIPA-*b*-PMCL copolymer (30 mg) in DMF (5 mL) was placed in a dialysis bag (MWCO = 3500) and dialyzed against deionized water at ambient temperature for 24 h. The water was replaced at 2 h intervals.

Measurements of size and size distribution

The size distribution of the micelles were estimated by a DLS using a particle-size analyzer (Zetasizer nano ZS, Malvern, UK) at 20°C. Scattered light intensity was detected at 90° to an incident beam. Measurements were made after the aqueous micellar solution (C = 0.3 g L^{-1}) was filtered with a microfilter having an average pore size of 0.2 μm (Advantec MFS). An average size distribution of aqueous micellar solution was determined based on CONTIN programs of Provencher and Hendrix.[20]

Observation on transmission electron microscope

Observation showed micelle morphology by TEM (JEM 1200-EXII, Tokyo, Japan). Drops of micelle solution (C = 0.3 g L^{-1}, no containing stain agent) were placed on a carbon film coated on a copper grid, and then dried at room temperature. The observation was conducted at an accelerating voltage of 100 kV.

Determining drug-loading content and drug entrapment efficiency

Using oil-in-water solvent evaporation, PNIPA-*b*-PMCL (50-fold CMC value) was dissolved in 6 mL

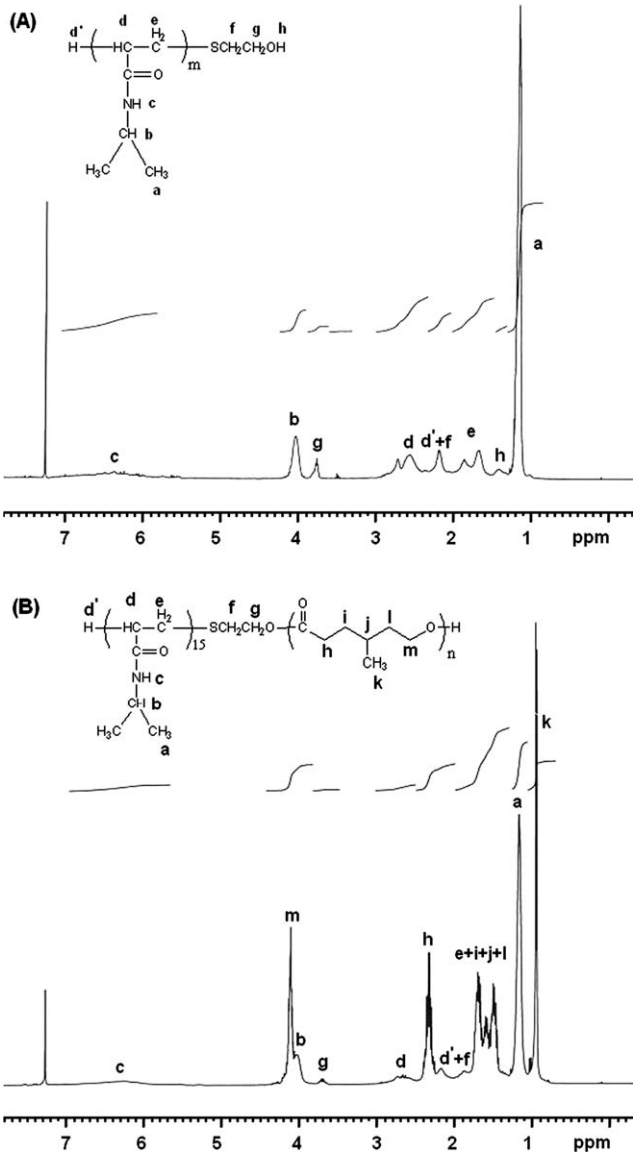

Figure 1 Representative ^{1}H-NMR spectroscopy of (A) PNIPA15, and (B) PNIPA15-*b*-PMCL18.

methylene chloride followed by adding anti-inflammatory drug indomethacin (IMC) with various weight ratios to the polymer (0.5/1–5/1) serving as a model drug. The solution was added dropwise to 150 mL distilled water containing 1 wt % poly(vinyl alcohol) under vigorous stirring. Poly(vinyl alcohol) was used as a surfactant to reduce micelle aggregation. Sonication reduced droplet size at ambient temperature for 60 min. The emulsion was stirred at ambient temperature overnight to evaporate the methylene chloride. The unloaded residue of IMC was removed by filtration using a Teflon filter (Whatman) with an average pore size of 0.45 μm. Vacuum drying obtained the micelles. A weighed amount of micelle was disrupted by adding a 10-fold excess volume of DMF. Drug content was assayed spectrophotometrically at 320 nm using a Diode Array UV-vis Spectrophotometer. Equations (1) and (2) calculate the drug-loading content and drug entrapment efficiency, respectively:

$$\text{Drug-loading content (\%)} = (\text{weight of drug in micelles/weight of micelles}) \times 100 \quad (1)$$

$$\text{Drug-entrapment efficiency (\%)} = (\text{weight of drug in micelles/weight of drug fed initially}) \times 100 \quad (2)$$

RESULTS AND DISCUSSION

Synthesis and characterization of the PNIPA-*b*-PMCL and PNIPA-*b*-PBCL copolymers

This study synthesized various amphiphilic PNIPA-*b*-PMCL and PNIPA-*b*-PBCL diblock copolymers by ring-opening polymerization of either MCL or BCL with hydroxyl-terminated macroinitiators PNIPA. The hydroxyl terminated PNIPA synthesized by radical chain-transfer polymerization of NIPA with ME as a chain-transfer agent (with the molar ratio 10/1, and 20/1) in the presence of BPO as the radical initiator in THF at 70°C for 24 h. Figure 1(A,A) show the ^{1}H-NMR and FTIR spectra of the PNIPA. The typical chemical shift of the PNIPA followed at $\delta = 3.78$ ppm (polymer end, $HOCH_2CH_2S$-PNIPA), 4.02 ppm (H_b, $-CH(CH_3)_2$), 1.08 ppm (H_a, $-CH(CH_3)_2$). Observations show the typical amide absorption bands of PNIPA at about 1650 (amide I band) and 1540 cm^{-1} (amide II band) in the FTIR spectrum. This work also calculated the degree of PNIPA

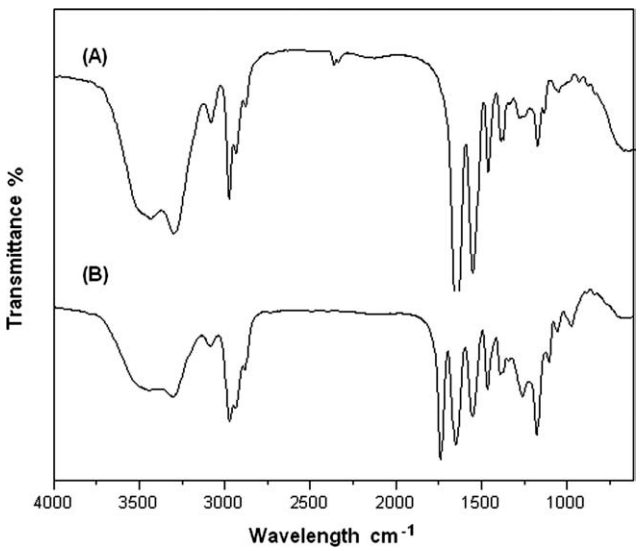

Figure 2 IR spectra of (A) PNIPA15, and (B) PNIPA15-*b*-PMCL18.

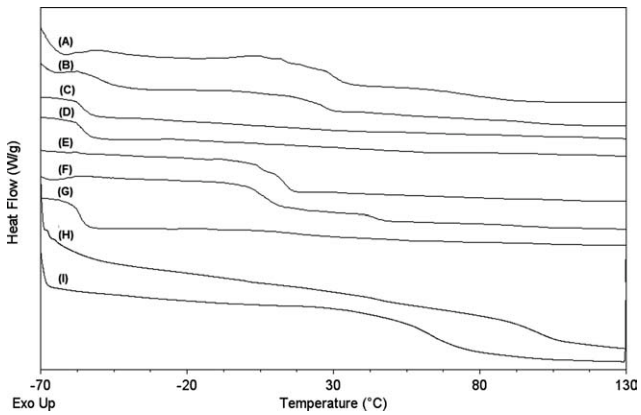

Figure 3 DSC curves of the control PNIPA15 (H), PNIPA7 (I), and PNIPA-*b*-PMCL with the molar ratio [PNIPA]/[MCL] (A) 15/9, (B) 15/18, (C) 15/32, (D) 15/45, (E) 7/46, and PNIPA -*b*-PBCL with the molar ratio [PNIPA]/[BCL] (F) 15/13, (G) 7/34, for second run.

polymerization using integration values. The $M_{n,\mathrm{NMR}}$ of PNIPA was 870, and 1800 g mol^{-1} with DP = 7, and 15, respectively. Scheme 1 illustrates the synthesis of amphiphilic PNIPA-*b*-PMCL and PNIPA-*b*-PBCL diblock copolymers. This research used the PNIPA hydroxyl group as the initiation site for ring-opening polymerization of MCL or BCL in the presence of $SnOct_2$ (1.5 wt %) as the catalyst in chlorobenzene at reflux for 24 h. With the fixed macroinitiator, copolymers with different compositions were prepared by changing the substituted comonomer MCL or BCL feed ratio. Table I compiles the results of polymerization. The yields between 45 and 80% were moderate. The 4-methyl or 4-phenyl substituted for ε-CL reduces polymerization rate, as also observed for other substituted lactones,[21,22] preventing the parent polymer from crystallizing. The M_ns of the block copolymers obtained from copolymerization of MCL (or BCL) and PNIPA increased with the increase of MCL (or BCL) molar ratios to PNIPA in the feed. When using the PNIPA15 as the macroinitiator, the molar ratios of MCL to PNIPA15 in feed increase from 15 to 70, the M_ns of the copolymer increased from 2330 to 6320 g mol^{-1} with M_w/M_n between 1.26 and 1.55, respectively. The molar ratio of block copolymers compositions was analyzed by ^{1}H-NMR. The amounts of comonomer incorporated into the copolymer were calculated from comparing the integral area of resonance peaks δ = 0.95 ppm of the methyl protons of PMCL with the resonance peaks δ = 1.19 ppm of dimethyl protons of PNIPA. From ^{1}H-NMR analysis, copolymerization of the monomers was lower than the corresponding feeds when the molar ratio of monomer in the feed was higher. This is probably because the substituted lactones polymerize significantly slower than ε-caprolactone, stemming from transesterification. At the same feed ratio, the BCL reactivity of polymerization was slower than the MCL. This suggests that conjugative effect and spatial hindrance of the phenyl group have a strong influence on polymerization.[23]

Figure 1(B) shows the typical ^{1}H-NMR spectrum of the block copolymer PNIPA15-*b*-PMCL18. This study assigns typical signals to the corresponding hydrogen atoms of the copolymers. Observations show typical signals of the PNIPA blocks at δ = 4.01 (H_b, —C*H*(CH$_3$)$_2$), 1.19 (H_a, —CH(C*H*$_3$)$_2$), 1.58–2.68 (H_d, H_e, —C*H*— and —C*H*$_2$—). The typical signals of PMCL blocks exhibit at δ = 4.11 (H_m, —C*H*$_2$OCO—), 2.31 (H_h, —OCOC*H*$_2$—), 1.38–1.81 (H_{i+j+l}, —C*H*$_2$C*H*C*H*$_2$—), 0.98 (H_k, —CH$_2$CH(C*H*$_3$)CH$_2$—). Figure 2(B) shows the FTIR spectrum of the PNIPA15-*b*-PMCL18, the characteristic band at about 1736 cm^{-1} (ν carbonyl) is associated with PMCL.

Table I and Figure 3 show the thermal behaviors and DSC curves of the PNIPA-*b*-PM(B)CL block copolymers. The thermal behaviors of the block copolymers are quite complicated and strongly dependent on the molecular weights of PM(B)CL and PNIPA segments, and the composition of copolymers.[23–25] According to DSC, PNIPA-*b*-PMCL and PNIPA-*b*-PBCL diblock copolymers exhibited only T_g, are amorphous. Fixing the length of the PNIPA block (PNIPA15) and increasing the length of PMCL and PBCL block, observations show a decrease in T_gs, which are lower than the PBCL (T_g = 18 °C)[26] and PMCL (T_g = −53 °C)[27] except the length of PMCL block below 18 units. As the length of PMCL or PBCL is smaller than the 13 unit, the PNIPA displayed a glass transition (T_{g2}) at 83.7°C (PNIPA15-*b*-PMCL9), and 44.7°C (PNIPA15-*b*-PBCL13), respectively, lower than the homo-PNIPA (T_g = 100°C of PNIPA15, and 63°C of PNIPA7) attribute to the hydrogen-bonding decrease as the PMCL or PBCL incorporated into the polymer. T_gs of PNIPA-*b*-PMCL and PNIPA-*b*-PBCL are higher than PNIPA-*b*-PCL. This is due to the steric hindrance of MCL containing the methyl substituents (or BCL containing the phenyl substituents) that reduce flexibility of backbone.

LCST behavior

This work characterizes LCST behaviors of PNIPA-*b*-PMCL and PNIPA-*b*-PBCL copolymers solutions by measuring their cloud points. Figure 4 shows the transmittance changes in PNIPA-*b*-PMCL and PNIPA-*b*-PBCL at different temperatures·LCST values for the PNIPA-*b*-PMCL aqueous solution were observed to shift to lower temperature than that for PNIPA homopolymers. The LCSTs were in the range of 33.7–36.3°C for PNIPA15-*b*-PMCLs lower than that of homo-PNIPA15 in water (about 43.1°C) and Table II summarizes the results. By decreasing PMCL block length, observations show sharper and more dominant transmittance reductions. Furthermore, when using the shorter PNIPA or PBCL, the transition was

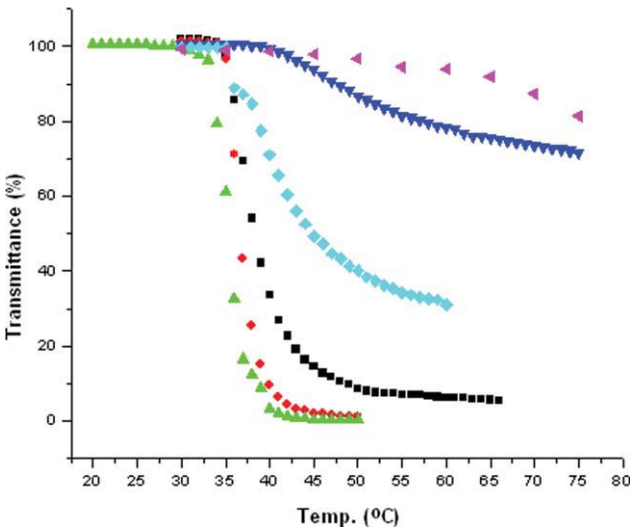

Figure 4 Phase-transition curves of PNIPA-*b*-PM(B)CL with varying compositions in the 0.2 wt % aqueous solution at λ = 500 nm. (▲; PNIPA15-*b*-PMCL9, ●; PNIPA15-*b*-PMCL22, ■; PNIPA15-*b*-PMCL18, ◇; PNIPA15-*b*-PMCL45, ▼; PNIPA7-*b*-PMCL46, ◤ PNIPA7-*b*-PBCL34). [Color figure can be viewed in the online issue, which is available at www.interscience.wiley.com.]

very weak, even in a higher temperature range. The lowest transmittance reached 70% for PNIPA7-*b*-PMCL46. The LCST behavior of PNIPA7-*b*-PBCL34 can even be lost. However, a contrary findings show that the LCST have slightly increased tendency with increasing MCL content. This may be attributed to the hydrophobic interaction and the hydrophobicity do not show any significant change.[28] These outcomes indicate that the hydrophilicity of the PNIPA block significantly affects the transition temperature of the corresponding copolymer, and that the chain length of the PMCL block did not notable influence the transition temperature.

Micelles of block copolymers

The amphiphilic nature of the block copolymers, consisting of hydrophilic PNIPA and hydrophobic PMCL (or PBCL) blocks, provides an opportunity to form micelles in water. This study investigates the characteristic of block copolymer micelles in an aqueous phase by fluorescence techniques. A fluorescence technique using pyrene as a probe determined critical micelle concentrations (CMCs) of the block copolymers in an aqueous phase.

Figure 5(A) shows the excitation spectra of pyrene in the PNIPA-*b*-PMCL solution with various concentrations. Findings show that fluorescence intensity increases with the increase in PNIPA-*b*-PMCL concentration. This work utilized the characteristic pyrene excitation spectra, a red shift of the (0,0) band from 334 to 337 nm upon pyrene partition into micellar hydrophobic core, to determine CMC values of the PNIPA-*b*-PMCL and PNIPA-*b*-PBCL block copolymers. Figure 5(B) shows the intensity ratios (I_{337}/I_{334}) of pyrene excitation spectra versus the logarithm of PNIPA-*b*-PMCL, and PNIPA-*b*-PBCL copolymer concentrations. This study determined the CMC from intersecting straight-line segments, drawn through the points at the lowest polymer concentrations, lying on a nearly horizontal line, with that going through the points on the rapidly rising part of the plot. Table II shows CMC values of the block copolymers dependent on block composition. At the fixed length of the hydrophilic block (PNIPA15), the CMC values of the copolymers PNIPA-*b*-PMCL reduced from 2.74 to 0.98 mg L^{-1}, with increasing hydrophobic PMCL chain length. The CMC values were much lower than those of low-molecular-weight surfactants and comparable with those of other polymeric amphiphilies.[29] Very low CMC values for PNIPA-*b*-PMCL, and PNIPA-*b*-PBCL copolymers indicate a very strong tendency of the diblock copolymers toward micelles formation in the aqueous solution. The length and steric hindrance of hydrophobic segment increased and the CMC values decreased. As the length of hydrophilic (PNIPA) segment increased, an increased CMC values exhibited. The CMC values of PNIPA-*b*-

TABLE II
Properties of IMC-Loaded PNIPA-*b*-PM(B)CL Micelles

Copolymer	CMC (mg/L)	Feed weight ratio IMC/polymer	Drug entrapment efficiency (%)	Drug loading content (%)	LCST[a] (°C)	Micelle size (nm)
PNIPA 15-*b*-PMCL9	2.74	0.5/1	62.5	41.6		
PNIPA 15-*b*-PMCL9	2.74	1/1	84.9	42.5	33.7	114.5 ± 48.2
PNIPA 15-*b*-PMCL9	2.74	2/1	93.4	31.1		
PNIPA 15-*b*-PMCL9	2.74	5/1	96.9	24.5		
PNIPA 15-*b*-PMCL18	1.21	1/1	93.8	46.9	35.1	192.2 ± 51.9
PNIPA 15-*b*-PMCL32	1.03	1/1	94.7	47.8	35.9	206.0 ± 53.5
PNIPA 15-*b*-PMCL45	0.98	1/1	98.8	49.4	36.3	207.0 ± 51.5
PNIPA 15-*b*-PBCL13	1.54	1/1	49.2	24.6	–	150.8 ± 31.0
PNIPA 7-*b*-PBCL34	0.29	1/1	84.9	42.5	67.0	93.6 ± 29.1
PNIPA 7-*b*-PMCL46	0.90	1/1	60.1	30.0	47.1	133.6 ± 37.7

[a] LCST was determined spectroscopically at 500 nm in 0.2 wt % aqueous polymer solution.

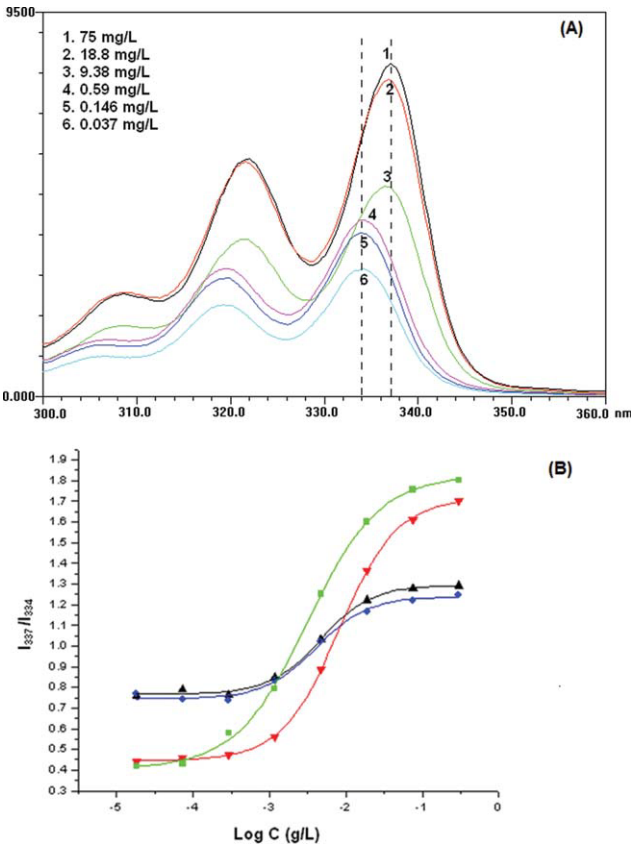

Figure 5 (A) Excitation spectra of the PNIPA15-*b*-PMCL45 copolymer monitored at $\lambda_{em} = 390$ nm (B) Plot of I_{337}/I_{334} intensity ratio (from pyrene excitation spectra; pyrene concentration $= 6.1 \times 10^{-7}$ *M*) versus the logarithm of concentration (log C) for (▼) PNIPA15-*b*-PBCL13, (■) PNIPA7-*b*-PBCL34, (▲) PNIPA15-*b*-PMCL45, and (●) PNIPA7-*b*-PMCL46 diblock copolymer ($\lambda_{em} = 390$ nm). [Color figure can be viewed in the online issue, which is available at www.interscience.wiley.com.]

PM(B)CLs were similar to the reported values of amphiphilc block copolymers such as MPEG-*b*-PM(B)CL, and poly(2-ethyl-2-oxazoline)-PCL block copolymers.[30,31]

The mean hydrodynamic diameters of micelles, measured by DLS, were in the range of 90–210 nm (Table II). Fixing the concentration at 50-fold CMC (50 × CMC) value, the mean diameter of micelles increased with increasing the length of hydrophobic segments. PNIPA7-*b*-PM(B)CL micelles were smaller than PNIPA15-*b*-PM(B)CL. This is attributed to have larger the hydrodynamic diameter when have longer the hydrophilic segment. These facts indicate that micelles' size depends on polymer composition: the length of the hydrophilic or hydrophobic segment in the chain and the steric hindrance of pendent groups in copolymer.[32] Figure 6 also show micelles morphology. Polymer compositions have a dramatic effect on micelle shape. Several of the interesting morphologies obtained with PNIPA-*b*-PM(B)CL copolymers include a rod-like, spherical, and vesicle structure. An increase in molecular weight of the core block, and a subsequent decrease in the block PNIPA weight fraction (W_{PNIPA}) to 0.17–0.13, results the shape transition from spherical to rod-like for PNIPA-*b*-PBCL copolymers and transition from vesicle to spherical for PNIPA-*b*-PMCL copolymers. These results were in good agreement with amphiphilic block copolymer systems which form crew cut aggregates to produce a wide range of morphologies.[33] The TEM picture of PNIPAM15-*b*-PMCL9 shows the formation of a vesicle-shaped micelle having a clear boundary. However, the micellar cores, composed of the longer hydrophobic PMCL block, appear as dark spheres in PNIPA7-*b*-PMCL46. If the length of the PNIPA is decreased, the degree of core stretching will increase, and at some point the morphology changes to produce rod shaped aggregates.[34] The PMCL block is much easier to form the vesicle than PBCL block. This is attributed to the strong hydrophobic repulsion of the phenyl groups in PBCL and PBCL is more hydrophobic than PMCL. As the hydrophobic content of the amphiphilic is increased through the addition of PBCL, micelles develop morphologies with decreasing interfacial curvature, namely the progression from vesicle to rod-like.

Evaluation of drug loading content and drug entrapment efficiency

This research measured drug-loading content and entrapment efficiency of polymeric micelles fabricated by an oil-in water solvent evaporation method with various IMC-to-polymer feed ratios by UV-vis absorption spectroscopy. IMC had a maximum absorption peak at 320 nm, proportional to concentration. After eliminating the unloaded precipitates of IMC, the amount of loaded IMC was determined by absorbance at 320 nm. Table II shows the calculated drug-loading content and entrapment efficiency values. The amount of IMC introduced into the micelle by controlling the weight ratio between drug and polymer. Drug entrapment efficiency increased with the weight ratio of drug to polymer. But, observations show a contradiction for drug-loading content. A possible explanation is that a higher drug loading results in an increased drug concentration gradient between the polymer matrix and the other aqueous phase, which in turn leads to more drug loss in the fabrication process. The polymer itself may have a limited capacity to encapsulate a specific drug. Beyond its maximum capacity, more drugs might be washed during the fabrication process. At the constant feed weight ratio (1/1), drug-loading content and entrapment efficiency increased up to 49.4 and 98.8 %, respectively, with the increased length of the PMCL block. However,

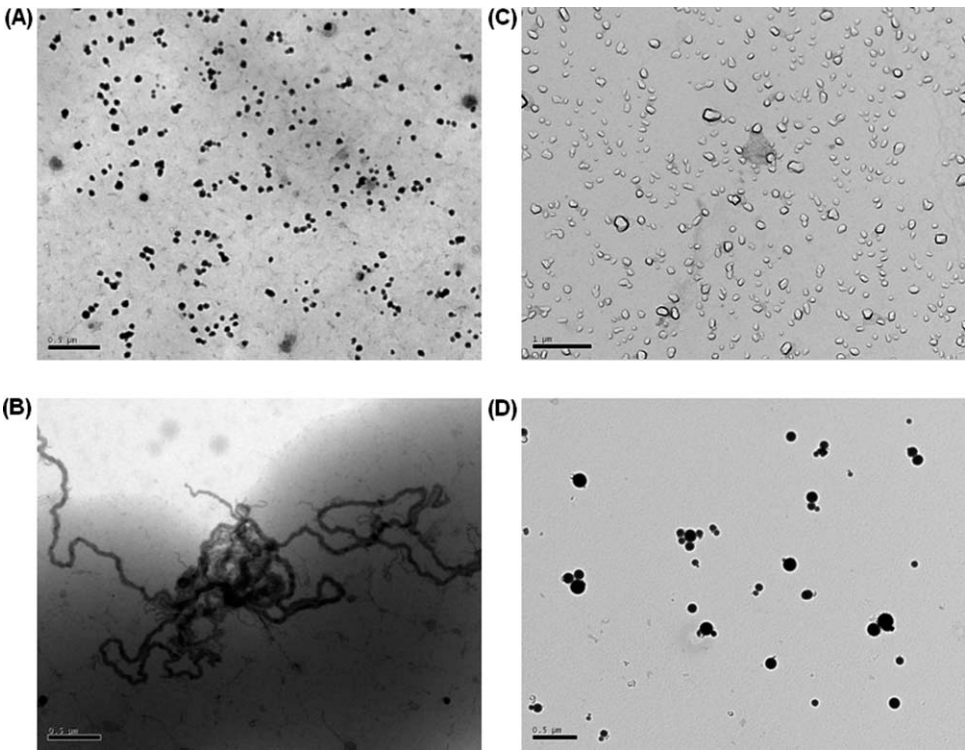

Figure 6 TEM photograph of the micelles formed by (A) PNIPA15-*b*-PBCL13 ($W_{PNIPA} = 0.54$), (B) PNIPA7-*b*-PBCL34 ($W_{PNIPA} = 0.17$), (C) PNIPA15-*b*-PMCL9 ($W_{PNIPA} = 0.63$), and (D) PNIPA7-*b*-PMCL46 ($W_{PNIPA} = 0.13$).

drug-loading content and entrapment efficiency dramatically decreased when steric hindrance of hydrophobic segment increased (for PNIPA15-*b*-PBCL13). These values strongly relate to the interaction parameter between the hydrophobic segment of the micelle and drug. This is because more steric hindrance in the hydrophobic segment in block copolymers hinders the amount of drug entrapped in the micelles.

CONCLUSIONS

This study successfully synthesizes thermal sensitive block copolymers PNIPA-b-PMCL and PNIPA-b-PBCL by ring-opening polymerization using the hydroxyl-terminated PNIPA as the ring-opening reagent. PNIPA-*b*-PMCL with LCST ranges from 33.7–36.3 °C lower than that of homo-PNIPA in water (PNIPA15 43.1°C). Increased length and steric hindrance of hydrophobic segment in an amphiphilic diblock copolymer produces lower CMC values. Drug entrapment efficiency and drug loading content increased with increased length of the hydrophobic block.

References

1. Gil, E. S.; Hudson, S. M. Prog Polym Sci 2004, 29, 1173.
2. Bae, Y. S.; Fukushina, S.; Harada, A.; Kataoka, K. Angew Chem Int Ed 2003, 42, 4640.
3. Nitschke, M.; Gramm, S.; Gotze, T.; Valtink, M.; Drichel, J.; Voit, B.; Engelmann, K.; Werner, C. J Biomed Mater Res 2007, 80, 1003.
4. Reppy, M. A.; Pindzola, B. A. Chem Commun 2007, 4317.
5. Tachibana, Y.; Kurisawa, M.; Uyama, H.; Kobayashi, S. Biomacromolecules 2003, 4, 1132.
6. Liu, X. M.; Wang, L. S. Biomaterials 2004, 25, 1929.
7. Cai, Y. L.; Tang, Y. Q.; Armes, S. P. Macromolecules 2004, 37, 9728.
8. Schild, H. G. Prog Polym Sci 1992, 17, 163.
9. Liu, S. Q.; Yang, Y. Y.; Liu, X. M.; Tong, Y. W. Biomacromolecules 2003, 4, 1784.
10. Kohori, F.; Sakai, K.; Aoyagi, T.; Yokoyama, M.; Yamato, M.; Sakurai, Y.; Okano, T. Colloids Surf B 1999, 16, 195.
11. Kohori, F.; Yokoyama, M.; Sakai, K.; Okano, T. J Controlled Release 2002, 78, 155.
12. Kohori, F.; Sakai, K.; Aoyagi, T.; Yokoyama, M.; Yamato, M.; Sakurai, Y.; Okano, T. J Controlled Release 1998, 55, 87.
13. Liu, S. Q.; Tong, Y. W.; Yang, Y. Y. Biomaterials 2005, 26, 5064.
14. Choi, C.; Chae, S. Y.; Nah, J. W. Polymer 2006, 47, 4571.
15. Nakayama, M.; Okano, T.; Miyazaki, T.; Kohori, F.; Sakai, K.; Yokoyama, M. J Controlled Release 2006, 115, 46.
16. Li, Y. Y.; Zhang, X. Z.; Cheng, H.; Zhu, J. L.; Li, U. N.; Cheng, S. X.; Zhuo, R. X. Nanotechnology 2007, 18, 505101.
17. Zupancich, J. A.; Bates, F. S.; Hillmyer, M. A. Macromolecules 2006, 39, 4286.
18. Vangeyte, P.; Jérôme, R. J Polym Sci Part A: Polym Chem 2004, 42, 1132.
19. Chang, C.; Wei, H.; Quan, C. Y.; Li, Y. Y.; Wang, Z. C.; Cheng, S. X.; Zhang, X. Z.; Zhuo, R. X. J Polym Sci Part A: Polym Chem 2008, 46, 3048.
20. Provencher, S. W.; Hendrix, J. J Phys Chem 1978, 69, 4237.
21. Mecerreyes, D.; Miller, R. D.; Hedrick, J. L.; Detrembleur, C.; Jérôme, R. J Polym Sci Part A: Polym Chem 2000, 38, 870.
22. Parrish, B.; Quansah, jk; Emrick, T. J Polym Sci Part A: Polym Chem 2002, 40, 1983.

23. Zou, T.; Li, S. L.; Zhang, X. Z.; Wu, X. J.; Cheng, S. X.; Zhuo, R. X. J Polym Sci Part A: Polym Chem 2007, 45, 5256.
24. Trollsås, M.; Kelly, M. A.; Claesson, H.; Siemens, R.; Hedrick, J. L. Macromolecules 1999, 32, 4917.
25. Lee, R. S.; Huang, Y. T. J Polym Sci Part A: Polym Chem 2008, 46, 4320.
26. Deng, X.; Yuan, M.; Cao, X.; Li, X. Macromol Chem Phys 2001, 202, 2417.
27. Seefried, C. G., Jr.; Koleske, J. V. J Polym Sci Polym Phys 1975, 13, 851.
28. Yin, X.; Stöver, H. D. H. Macromolecules 2002, 35, 10178.
29. Shim, I. G.; Kim, S. Y.; Lee, Y. M.; Cho, C. S.; Sung, Y. K. J Controlled Release 1998, 51, 1.
30. Lee, R. S.; Hung, C. B. Polymer 2007, 48, 2605.
31. Lee, S. C.; Chang, Y.; Yoon, J. S.; Kim, C.; Kwon, Y. H. Macromolecules 1998, 32, 1847.
32. Vangeyte, P.; Gautier, S.; Jérôme, R. Colloids Surf A: Physicochem Eng Aspects 2004, 242, 203.
33. Allen, C.; Maysinger, D.; Eisenberg, A. Colloids Surf B 1999, 16, 3.
34. Zhang, L.; Eisenberg, A. J Am Chem Soc 1996, 118, 3168.